Dynamics of Fission Modes Studied with the 3-dimensional Langevin Equation

T. Ichikawa,* T. Asano, T. Wada, and M. Ohta

Department of Physics, Konan University, Kobe 658-8501, Japan

We investigate fission modes of ^{270}Sg with 3-dimensional Langevin equation. The shell correction energy is included in the total energy. The mass distribution and the total kinetic energy (TKE) distribution of fission fragments are calculated and are compared with the experimental results. Mass asymmetric fission dominates in the mode with the lower TKE, which is in agreement with the experimental result. The dynamics from saddle to scission is also discussed.

1. Introduction

In the heavy compound nucleus with $A > 200$, fission modes have been investigated from the measurement of the mass and the total kinetic energy (TKE) distribution at low excitation energy and the effect of shell energy are established well. At low excitation energy, the asymmetric fission mode is observed for all nuclei with $A > 200$.

For example, the measurement of the mass-energy distribution of the fission fragments of ^{270}Sg ($Z = 106$) was performed by Itkis et al.[1] It was observed that at low excitation energy, the mass asymmetric fission dominates in the components of the mode having lower TKE, whereas this tendency vanishes at high excitation case. The domination of the mass asymmetric fission in the components having low TKE is the characteristic of the nuclei heavier than the fermium region. From these results, the existence of the different dynamical fission paths was pointed out.

The problem of fission modes has also been studied theoretically. For example, Pashkevich calculated the energy surface in the multi-dimensional parameter space including the shell energy and found several saddle points and fission valleys.[2] However, it was a static calculation and was not sufficient to understand the mass-energy distribution. In order to understand these phenomena, the effect of the shell correction energy to the dynamical fission path is essential.

Therefore, we investigate fission modes from the mass and TKE distribution calculated with the 3-dimensional Langevin equation and investigate the influence of dynamics from saddle to scission. At the high excitation energy where the shell effect vanishes, the fission process has been studied on the basis of the fluctuation-dissipation dynamics and the Langevin equation[3] has been used to describe this dynamics. The 3-dimensional Langevin calculation agreed with experimental values of the mass distribution and the total kinetic energy of fission fragments. In this study, including the shell correction energy, we extend the 3-dimensional Langevin calculation to the case of the low excitation.

In this paper, we investigate fission modes of ^{270}Sg system and present results of the calculation of the mass distributions and the total kinetic energy of fission fragments. The influence of the potential energy on the dynamics is also discussed.

2. Framework

The shape of nucleus is described by the Two-Center parametrization and Figure 1 shows various shapes of ^{270}Sg with this parametrization. Z_0 denotes the distance between the harmonic oscillators in the unit of the radius of the spherical compound nuclei ($R_0 = r_0 (A_1 + A_2)^{1/3}$), δ denotes the deformation of the fragments with the constraint that both fragments have

same deformation ($\delta_1 = \delta_2$), and α denotes the mass asymmetry parameter ($\alpha = (A_1 - A_2)/(A_1 + A_2)$), where A_1 and A_2 are the mass number of the fragments. The liquid drop energy, the surface energy, and the coulomb energy are also calculated with this parametrization.

We describe the fission process by the following equation, called as the Langevin equation,

$$\frac{dq_i}{dt} = \left(m^{-1}\right)_{ij} p_j ,$$
$$\frac{dp_i}{dt} = -\frac{\partial V}{\partial q_i} - \frac{1}{2}\frac{\partial}{\partial q_i}\left(m^{-1}\right)_{jk} p_j p_k$$
$$- \gamma_{ij}\left(m^{-1}\right)_{jk} p_k + g_{ij} R_j(t), \qquad (1)$$

where the suffix stands for Z_0, δ, or α. Summation over repeated indices is implied. $V(q)$ is the potential energy taken account of shell effect, $m_{ij}(q)$ and $\gamma_{ij}(q)$ are the shape dependent collective inertia and dissipation tensors. We assume the random forces as the white noise type of which the normalized random force $R(t)$ is to satisfy $\langle R(t)\rangle = 0$, $\langle R_i(t_1)R_j(t_2)\rangle = 2\delta_{ij}\delta(t_1 - t_2)$. The strength of random force g_{ij} is calculated from $\gamma_{ij} T = g_{ik} g_{kj}$ that is given by the fluctuation-dissipative theorem. T denotes the temperature of the compound nucleus that is defined as $E^* = aT^2$ with the excitation energy of compound nucleus and the level density parameter a of Töke and Swiatecki.[4] The inertia tensor is calculated using the hydrodynamical model with Werner-Wheeler approximation[5] for the velocity field, and wall-and-window one-body dissipation[6] is adopted for the dissipation tensor.

The shell correction energy of the two-center shell model is calculated with the code TWOCTR.[7,8] The shell correction energy depends on the temperature of the nucleus. The temperature dependent factor of the shell correction energy is assumed as $\exp\left(-E^*/E_d\right)$, where E^* is the excitation energy and E_d is
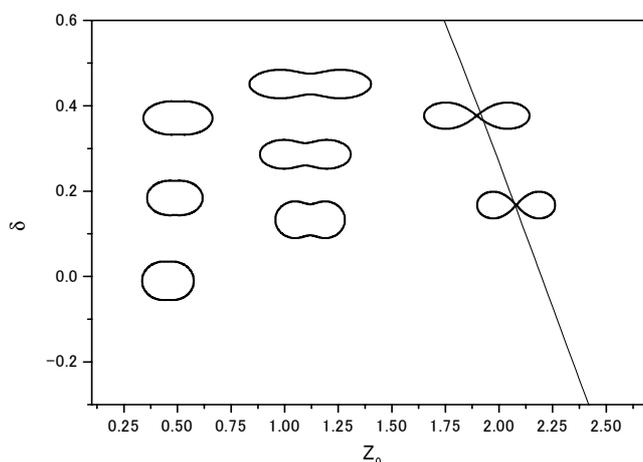

Figure 1. The various shapes with the Two-Center parametrization in the Z_0-δ plane.

*Corresponding author. E-mail: dn021001@center.konan-u.ac.jp. FAX: +81-78-435-2539.
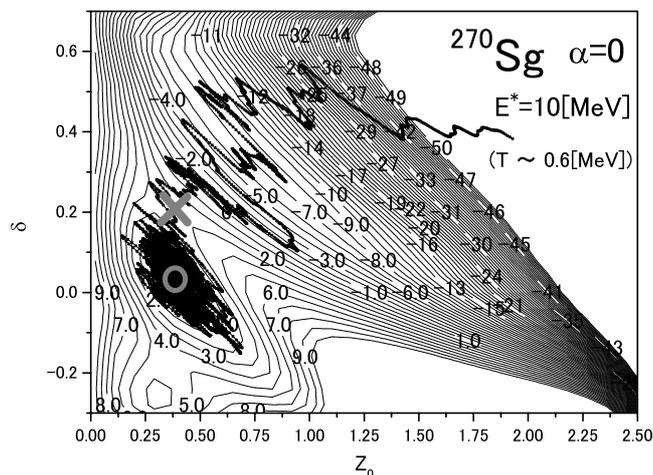
Figure 2. The landscape of this figure shows the total energy projected to Z_0-δ plane of ^{270}Sg. The circle denotes the ground state of compound nucleus and the cross denotes the first saddle point in the case of $\alpha = 0$. The line with dot is the sample trajectory of the calculation.
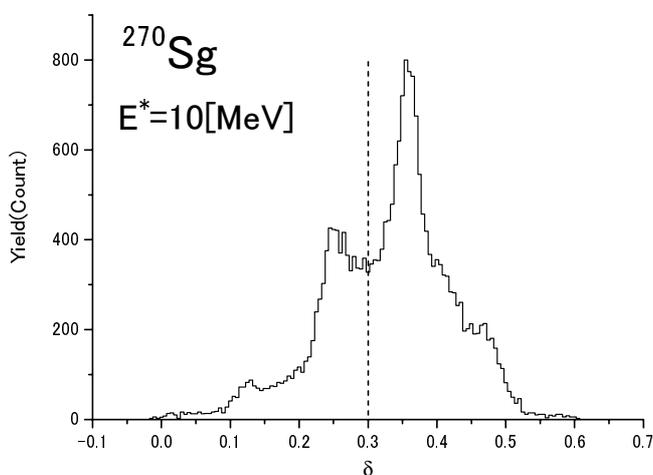

Figure 3. The distribution of the deformation of fission fragments at scission.

the shell damping energy that is taken to be 20 MeV.[9]

Figure 2 shows the potential landscape of ^{270}Sg at $E^* = 10$ MeV in the case of $\alpha = 0$. The circle denotes the ground state of this system and is the start point of the Brownian particle in Langevin calculation. The cross at $Z_0 = 0.3$ and $\delta = 0.2$ in Figure 2 indicates the first saddle of this system in the case of $\alpha = 0$.

3. Numerical Result

We investigate fission modes of the compound nucleus ^{270}Sg in the case that the excitation energy E^* is 10 MeV ($T \sim 0.6$ MeV). In this system, the fission barrier height B_f is approximately 5 MeV.

The histogram in Figure 3 shows the distribution of the deformation of fission fragments. In this figure, two peaks can be seen clearly at $\delta = 0.25$ and 0.36. From this result, we found that different dynamical fission paths exist.

The histogram in Figure 4 shows the distribution of the TKE of fission fragments. In this figure, different from Figure 3, it is not apparent that this distribution consists of several components. However, it is found that this TKE distribution cannot be fitted by a single Gaussian. According to the result that is shown in Figure 3, we divide the events of the fission fragments into two parts: one is the events with the deformation of fragments being $\delta > 0.3$ and the other is that with $\delta < 0.3$. In Figure 4, the dashed line denotes the TKE distribution of the events with $\delta > 0.3$ and the dotted line denotes that with $\delta < 0.3$. We found that the TKE of fragments with $\delta > 0.3$ is smaller than that with
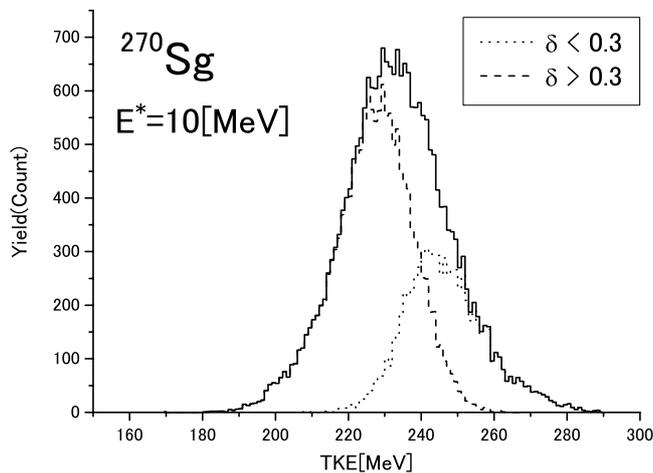

Figure 4. The distribution of the total kinetic energy of fission fragments. The dashed line denotes the TKE distribution for $\delta > 0.3$. The dotted line denotes the case of $\delta < 0.3$.
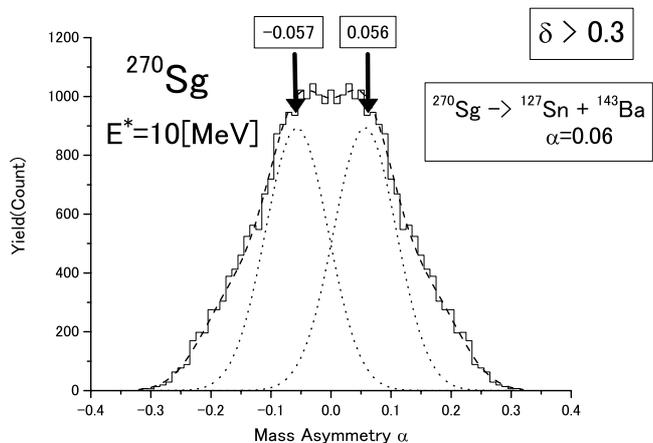

Figure 5. The distribution of the mass asymmetry of fission fragments with the deformation $\delta > 0.3$. The dashed line denotes the one fitted with four Gaussians and the dotted lines denote the main components of the fit.

$\delta < 0.3$. Fragments with lower TKE have larger deformation. It is seen that the TKE distribution with $\delta > 0.3$ has a simple peak structure and can be expressed as a single Gaussian. We expect that the distribution with $\delta > 0.3$ is from a single mode. As for components with $\delta < 0.3$, the statistical frequency is low compared with that with $\delta > 0.3$. We expect from Figure 3 that the events with $\delta < 0.3$ contain the contribution from the distribution that has a peak around $\delta \sim 0.36$. Since we still cannot extract a single mode from the components with $\delta < 0.3$, we investigate the mass distribution only for the events with $\delta > 0.3$ in this study.

The histogram of Figure 5 shows the distribution of the mass asymmetry α of fission fragments with $\delta > 0.3$. The dashed line is the result of the fitting with four Gaussians and the dotted lines are the main Gaussian components that are used in the fitting. From this result, the asymmetric fission can be seen clearly. Peaks of the main Gaussian components are at $\alpha = 0.056$ and -0.057.

The experimental results show that the mass asymmetric fission dominates in the mode having lower TKE distribution. Itkis et al.[1] proposed that the reaction of ^{270}Sg $\rightarrow$ ^{127}Sn + ^{143}Ba corresponding to Standard II mode was the main fission channel due to the effect of the deformed shell ($Z = 56$) and this reaction corresponds to $\alpha = 0.06$. We consider that our calculation results correspond to this experimental one. However, the peak energy of the TKE distribution in our calculation is larger than that of the experiment by about 30 MeV. At present stage, this difference is yet to be clarified.

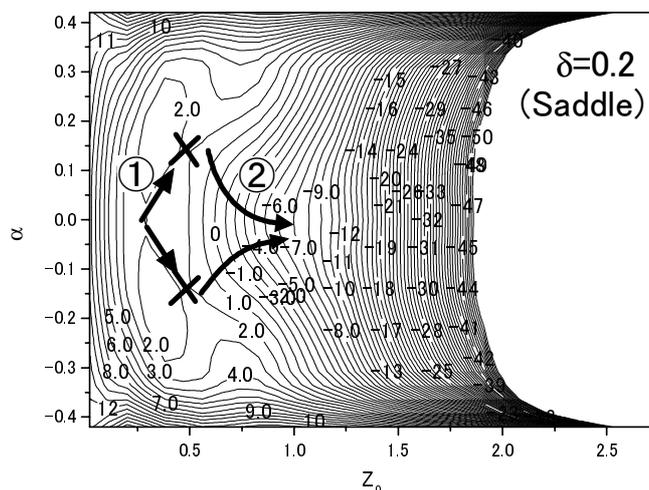Next, we consider the origin of this mass asymmetric dis-

Figure 6. The energy landscape of ^{270}Sg projected to Z_0-α in the case of the deformation $\delta = 0.2$.

Figure 7. The energy landscape of ^{270}Sg projected to Z_0-α in the case of the deformation $\delta = 0.36$.

tribution. Although the dynamical motion is calculated in the three-dimensional parameter space, it is instructive to look at the potential surface that are projected onto two-dimensional spaces like Z_0-α and Z_0-δ. Figure 6 shows the potential projected to Z_0-α at $\delta = 0.2$ that corresponds to the saddle point deformation in Z_0-δ plane of Figure 1. Figure 7 shows the potential projected to Z_0-α at $\delta = 0.36$ that corresponds to the maximum of the distribution in Figure 3. In the Z_0-α plane, the saddle point locates around at $Z_0 = 0.5$ and $\alpha = \pm 0.15$. First, in Figure 6, when fissioning nucleus goes from the ground state to the saddle point according to potential surface, the mass asymmetry α increases (the arrow 1). After passing through the saddle point (the cross), the fissioning nucleus goes toward scission and Z_0 and δ increase. At the same time, α decreases following the potential slope as shown by the arrow 2 in Figure 6. As is seen from the sample trajectory in Figure 2, after passing through the saddle point, the deformation δ increases from 0.2 to 0.4 with large fluctuation (around the number 3) while the increase of Z_0 is relatively small. With the increase of δ, the bump due to the shell effect becomes prominent at $Z_0 = 0.75$ and $\alpha = 0$ in Figure 7. Since the Brownian particle keeps away from this bump, the mass asymmetry α increases again (the arrow 4) and the fission nucleus goes to asymmetric direction. This is how the asymmetry of fission fragments is determined.

It should be noted that the potential around $Z_0 = 1.2 \sim 1.5$ is very flat in α direction in the present system. In addition, the mass asymmetry α at the scission point differs from the one at the saddle point. Therefore, it is inappropriate to determine the mass asymmetry α by the potential valley; the dynamics after the saddle point plays a very important role for the determination of the mass asymmetry at scission. The mass asymmetry distribution cannot be estimated only from the position of the saddle point such as the discussion with the static calculation. Thus, the dynamical calculation is very important for the understanding of the fission modes.

4. Summary

We studied the problem of fission mode by using the 3-dimensional Langevin equation on the basis of the fluctuation-dissipation dynamics and discussed the mass and the TKE distribution.

The static calculation in which the potential energy is calculated such as the works by Pashkevich is not sufficient to understand the mass-energy distribution. The dynamical calculation that takes account of the shell effect is needed in order to under-
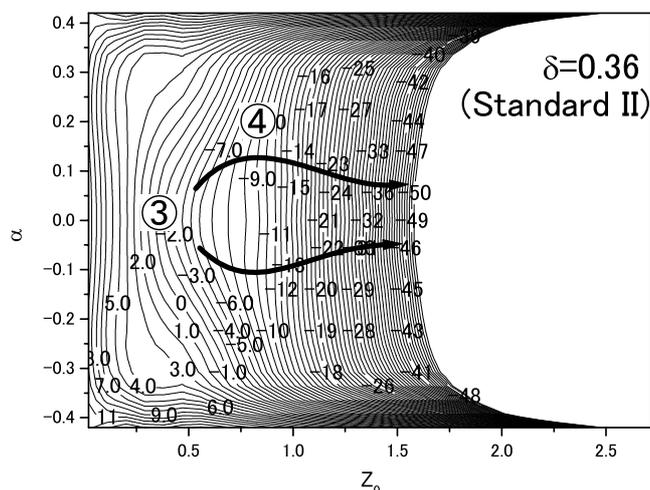
stand fission paths. We solved the 3-dimensinal Langevin equation numerically in the potential energy including the shell correction and investigated fission modes for the system of ^{270}Sg.

From the calculation results, we clearly found two fission modes. The one of these fission modes corresponds to the Standard II mode that has large deformation and has lower TKE. In the mass distribution of the fission fragments of this mode, the mass asymmetric fission dominates. This result is in qualitative agreement with the experimental one. However, the peak energy of the TKE distribution of the fission fragments is larger than the experimental result by about 30 MeV and this point is yet to be clarified.

We also investigated the influence of the potential energy on the dynamics to understand the result of the mass asymmetric distribution. We found that the mass asymmetry at the scission is determined by the dynamics after the saddle rather than the position of the saddle point. Therefore, we conclude that in order to understand fission modes, the dynamical calculation is very important.

As a future study, we need the 4-dimensional Langevin calculation taking account of the independent deformation of each fragment in order to include the deformed shell effect. It is also necessary to include the change of the nuclear temperature due to the particle emission. These studies are now under progress.

References

(1) M. G. Itkis, N. A. Kondratiev, E. M. Kozulin, Yu. Ts. Oganessian, I. V. Pokrovsky, and E. V. Prokhorova, Phys. Rev. C **59**, 3172 (1999).
(2) V. V. Pashkevich, Nucl. Phys. Prog. A **169**, 275 (1971).
(3) T. Wada, Y. Abe, and N. Carjan, Phys. Rev. Lett. **70**, 3538 (1993).
(4) J. Töke and W. J. Swiatecki, Nucl. Phys. A **372**, 141 (1981).
(5) H. J. Krappe, J. R. Nix, and A. J. Sierk, Phys. Rev. C **20**, 992 (1979).
(6) J. R. Nix and A. J. Sierk, Phys. Rev. C **15**, 2072 (1977).
(7) S. Suekane, A. Iwamoto, S. Yamaji, and K. Harada, JAERI-memo 5918 (1974).
(8) A. Iwamoto, S. Yamaji, S. Suekane, and K. Harada, Prog. Theor. Phys. **55**, 115 (1976).
(9) A. V. Ignatyuk, G. N. Smirenkin, and A. S. Tishin, Sov. J. Nucl. Phys. **21**, 255 (1975).